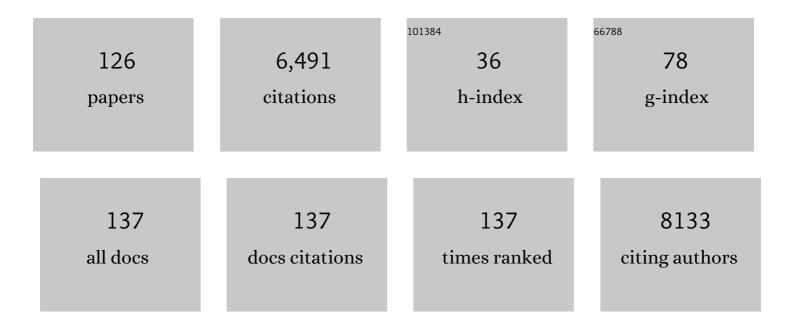
List of Publications by Year in descending order

Source: https://exaly.com/author-pdf/8969829/publications.pdf Version: 2024-02-01



DONG HWAN WANG

#	Article	IF	CITATIONS
1	Gamma–ray irradiation of lead iodide precursor for enhanced perovskite crystalline properties. Applied Surface Science, 2022, 571, 151263.	3.1	3
2	Mesoporous Trap of Molecular Sieves via Water-Selective Capture for Stable Perovskite Quantum Dots. ACS Sustainable Chemistry and Engineering, 2022, 10, 1115-1124.	3.2	5
3	Recent progress in organic solar cells based on non-fullerene acceptors: materials to devices. Journal of Materials Chemistry A, 2022, 10, 3255-3295.	5.2	105
4	Electrode stress passivation via oxide titanium amorphous interlayer for flexible non-fullerene organic photovoltaics. Organic Electronics, 2022, 102, 106438.	1.4	1
5	Physical engineering of antiâ€solvents in perovskite precipitation for enhanced photosensitive affinity. International Journal of Energy Research, 2022, 46, 9748-9760.	2.2	3
6	Suppressed oxidation in organic photovoltaics via hydrogen-bonded polyurethane acrylate resin encapsulation. Journal of Power Sources, 2022, 528, 231206.	4.0	2
7	Loosening effect of perovskite intermolecular exchanger with strong steric hindrance for highly sensitive photodetector. Applied Surface Science, 2022, 591, 153207.	3.1	5
8	Tris(4-(1-phenyl-1 <i>H</i> -benzo[<i>d</i>]imidazole)phenyl)phosphine oxide for enhanced mobility and restricted traps in photovoltaic interlayers. Journal of Materials Chemistry C, 2021, 9, 3642-3651.	2.7	2
9	High-Valent Iodoplumbate-Rich Perovskite Precursor Solution <i>via</i> Solar Illumination for Reproducible Power Conversion Efficiency. Journal of Physical Chemistry Letters, 2021, 12, 1676-1682.	2.1	12
10	Strong dark current suppression in flexible organic photodetectors by carbon nanotube transparent electrodes. Nano Today, 2021, 37, 101081.	6.2	50
11	Morphology Inversion of a Nonâ€Fullerene Acceptor Via Adhesion Controlled Decal oating for Efficient Conversion and Detection in Organic Electronics. Advanced Functional Materials, 2021, 31, 2103705.	7.8	15
12	A Facile and Effective Ozone Exposure Method for Wettability and Energy-Level Tuning of Hole-Transporting Layers in Lead-Free Tin Perovskite Solar Cells. ACS Applied Materials & Interfaces, 2021, 13, 42935-42943.	4.0	10
13	Formulation of conductive nanocomposites by incorporating silverâ€doped carbon quantum dots for efficient charge extraction. International Journal of Energy Research, 2021, 45, 21324-21339.	2.2	5
14	Versatile Pendant Polymer for Selective Charge Carrier Transport via Controlling the Supramolecular Selfâ€Assembly. ChemSusChem, 2021, 14, 5167-5178.	3.6	6
15	Molecular manipulation of PEDOT:PSS for efficient hole transport by incorporation of N-doped carbon quantum dots. Dyes and Pigments, 2021, 194, 109610.	2.0	12
16	One-step formation of core/shell structure based on hydrophobic silane ligands for enhanced luminescent perovskite quantum dots. Journal of Alloys and Compounds, 2021, 886, 161347.	2.8	12
17	Fully Inorganic CsSnI ₃ -Based Solar Cells with >6% Efficiency and Enhanced Stability Enabled by Mixed Electron Transport Layer. ACS Applied Materials & Interfaces, 2021, 13, 1345-1352.	4.0	30
18	Versatile Pendant Polymer for Selective Charge Carrier Transport via Controlling the Supramolecular Selfâ€Assembly. ChemSusChem, 2021, 14, 5078.	3.6	0

#	Article	IF	CITATIONS
19	Chelating Agent Mediated Sol–Gel Synthesis for Efficient Hole Extracted Perovskite Photovoltaics. Journal of Physical Chemistry C, 2020, 124, 25184-25195.	1.5	5
20	Superior Noise Suppression, Response Time, and Device Stability of Nonâ€Fullerene System over Fullerene Counterpart in Organic Photodiode. Advanced Functional Materials, 2020, 30, 2001402.	7.8	42
21	Hydrogenerated black titanium dioxide-embedded conducting polymer for boosting electron flow in perovskite devices. Journal of Alloys and Compounds, 2020, 846, 156329.	2.8	3
22	Light-Emitting Transistors with High Color Purity Using Perovskite Quantum Dot Emitters. ACS Applied Materials & Interfaces, 2020, 12, 35175-35180.	4.0	18
23	A gold nanodot array imprinting process based on solid-state dewetting for efficient oxide-free photovoltaic devices. Applied Physics Letters, 2020, 117, .	1.5	2
24	Metallic amorphous alloy for long-term stable electrodes in organic sensors and photovoltaics. Organic Electronics, 2020, 84, 105811.	1.4	2
25	Highly conductive PEDOT:PSS electrode obtained via post-treatment with alcoholic solvent for ITO-free organic solar cells. Journal of Industrial and Engineering Chemistry, 2020, 86, 205-210.	2.9	19
26	Solution-processable porous organic polymer for tailoring the charge transport property of planar perovskite solar cells. Dyes and Pigments, 2020, 178, 108332.	2.0	6
27	Acidity Suppression of Hole Transport Layer via Solution Reaction of Neutral PEDOT:PSS for Stable Perovskite Photovoltaics. Polymers, 2020, 12, 129.	2.0	21
28	Selective UV Absorbance of Copper Chalcogenide Nanoparticles for Enhanced Illumination Durability in Perovskite Photovoltaics. ACS Sustainable Chemistry and Engineering, 2020, 8, 7617-7627.	3.2	6
29	Highly dispersible graphene oxide nanoflakes in pseudo-gel-polymer porous separators for boosting ion transportation. Carbon, 2020, 166, 427-435.	5.4	10
30	Enhanced colloidal stability of perovskite quantum dots via split-ligand re-precipitation for efficient bi-functional interlayer in photovoltaic application. Journal of Industrial and Engineering Chemistry, 2020, 88, 137-147.	2.9	15
31	An unusual charge transfer accelerator of monomolecular Cb-OMe		

#	Article	IF	CITATIONS
37	Tailoring solubility of methylammonium lead halide with non-stoichiometry molar ratio in perovskite solar cells: Morphological and electrical relationships for high current generation. Solar Energy Materials and Solar Cells, 2019, 192, 24-35.	3.0	13
38	The Investigation of the Seebeck Effect of the Poly(3,4-Ethylenedioxythiophene)-Tosylate with the Various Concentrations of an Oxidant. Polymers, 2019, 11, 21.	2.0	10
39	Enhanced interface of polyurethane acrylate via perfluoropolyether for efficient transfer printing and stable operation of PEDOT:PSS in perovskite photovoltaic cells. Applied Surface Science, 2019, 467-468, 168-177.	3.1	9
40	Covalent organic nanosheets for effective charge transport layers in planar-type perovskite solar cells. Nanoscale, 2018, 10, 4708-4717.	2.8	31
41	Rapid Formation of a Disordered Layer on Monoclinic BiVO ₄ : Coâ€Catalystâ€Free Photoelectrochemical Solar Water Splitting. ChemSusChem, 2018, 11, 933-940.	3.6	34
42	Increased omnidirectional light absorbance by using hollow silica nanoparticles in an anti-reflective pattern for efficient organic photovoltaic devices. Organic Electronics, 2018, 53, 315-319.	1.4	1
43	Oxygen Contribution for Uniform Formation of Crystalline Zinc Oxide/Polyethylenimine Interfaces to Boost Charge Generation/Transport in Inverted Organic Solar Cells. Journal of Industrial and Engineering Chemistry, 2018, 61, 314-320.	2.9	2
44	Alignment of Cascaded Band-Gap via PCBM/ZnO Hybrid Interlayers for Efficient Perovskite Photovoltaic Cells. Macromolecular Research, 2018, 26, 472-476.	1.0	16
45	Thermally stable propanethiol–ligand exchanged Ag nanoparticles for enhanced dispersion in perovskite solar cells via an effective incorporation method. Journal of Industrial and Engineering Chemistry, 2018, 61, 71-77.	2.9	8
46	Work function optimization of vacuum free top-electrode by PEDOT:PSS/PEI interaction for efficient semi-transparent perovskite solar cells. Solar Energy Materials and Solar Cells, 2018, 176, 435-440.	3.0	36
47	Facile Synthetic Route of a Solution-Processable, Thieno[3,4-c]pyrrolo-4,6-dione-Based Conjugated Small Molecule and Control of the Optoelectronic Properties via Processing Additives. Applied Sciences (Switzerland), 2018, 8, 2644.	1.3	1
48	Facile NiOx Sol-Gel Synthesis Depending on Chain Length of Various Solvents without Catalyst for Efficient Hole Charge Transfer in Perovskite Solar Cells. Polymers, 2018, 10, 1227.	2.0	10
49	Long-Term Stable Transferred Organic Photoactive Layer-Based Photodiode with Controlled Wetting through Interface Stabilization. ACS Applied Materials & Interfaces, 2018, 10, 38603-38609.	4.0	6
50	Controlling the optoelectronic properties of narrow bandgap organic chromophores upon isoelectronic bridgehead substitution. Dyes and Pigments, 2018, 158, 233-239.	2.0	5
51	Tuning surface chemistry and morphology of graphene oxide by Î ³ -ray irradiation for improved performance of perovskite photovoltaics. Carbon, 2018, 139, 564-571.	5.4	24
52	Vacuum-process-based dry transfer of active layer with solvent additive for efficient organic photovoltaic devices. Journal of Materials Chemistry C, 2017, 5, 1106-1112.	2.7	9
53	Effect of vacuum treatment in diketopyrrolopyrrole (DPP) based copolymer with ratio controlled toluene- and benzene- functional groups for efficient organic photovoltaic cells: Morphological and electrical contribution. Organic Electronics, 2017, 46, 183-191.	1.4	6
54	A graphene-phthalocyanine hybrid as a next photoactive layer. Carbon, 2017, 119, 476-482.	5.4	12

#	Article	IF	CITATIONS
55	Interface engineering on phenanthrocarbazole/thienopyrroledione-based conjugated polymer for efficient organic photovoltaic devices with ideal nano-morphology and improved charge carrier dynamics. Dyes and Pigments, 2017, 145, 29-36.	2.0	4
56	Dry-Stamping-Transferred PC71BM Charge Transport Layer via an Interface-Controlled Polyurethane Acrylate Mold Film for Efficient Planar-Type Perovskite Solar Cells. ACS Applied Materials & Interfaces, 2017, 9, 15623-15630.	4.0	15
57	Water Splitting Progress in Tandem Devices: Moving Photolysis beyond Electrolysis. Advanced Energy Materials, 2016, 6, 1600602.	10.2	268
58	Morphology fixing agent for [6,6]-phenyl C ₆₁ -butyric acid methyl ester (PC ₆₀ BM) in planar-type perovskite solar cells for enhanced stability. RSC Advances, 2016, 6, 51513-51519.	1.7	10
59	Dramatically enhanced performances and ideally controlled nano-morphology via co-solvent processing in low bandgap polymer solar cells. Organic Electronics, 2016, 34, 42-49.	1.4	16
60	Counterbalancing of morphology and conductivity of poly(3,4-ethylenedioxythiophene) polystyrene sulfonate based flexible devices. Nanoscale, 2016, 8, 19557-19563.	2.8	13
61	PVdF-HFP/exfoliated graphene oxide nanosheet hybrid separators for thermally stable Li-ion batteries. RSC Advances, 2016, 6, 80706-80711.	1.7	24
62	Morphological engineering via processing additive in thin film bulk-heterojunction photovoltaic cells: A systematic understanding of crystal size and charge transport. Current Applied Physics, 2016, 16, 1424-1430.	1.1	8
63	Nanopatterned bulk-heterojunction photovoltaic cells using polyurethane acrylate (PUA) film replica of colloidal crystal arrays via stamping transfer process. Macromolecular Research, 2016, 24, 483-487.	1.0	1
64	Self-Position of Au NPs in Perovskite Solar Cells: Optical and Electrical Contribution. ACS Applied Materials & amp; Interfaces, 2016, 8, 449-454.	4.0	91
65	Large Area Platinum and Fluorine-doped Tin Oxide-free Dye sensitized Solar Cells with Silver-Nanoplate Embedded Poly(3,4-Ethylenedioxythiophene) Counter Electrode. Electrochimica Acta, 2016, 187, 218-223.	2.6	10
66	Hydrophilic polyurethane acrylate and its physical property for efficient fabrication of organic photovoltaic cells via stamping transfer. Organic Electronics, 2016, 31, 295-302.	1.4	6
67	Surface-Engineered Graphene Quantum Dots Incorporated into Polymer Layers for High Performance Organic Photovoltaics. Scientific Reports, 2015, 5, 14276.	1.6	56
68	A Mechanistic Understanding of a Binary Additive System to Synergistically Boost Efficiency in All-Polymer Solar Cells. Scientific Reports, 2015, 5, 18024.	1.6	37
69	Facile control of intra- and inter-particle porosity in template-free synthesis of size-controlled nanoporous titanium dioxides beads for efficient organic–inorganic heterojunction solar cells. Journal of Power Sources, 2015, 279, 72-79.	4.0	6
70	Unassisted photoelectrochemical water splitting beyond 5.7% solar-to-hydrogen conversion efficiency by a wireless monolithic photoanode/dye-sensitised solar cell tandem device. Nano Energy, 2015, 13, 182-191.	8.2	138
71	Conflicted Effects of a Solvent Additive on PTB7:PC ₇₁ BM Bulk Heterojunction Solar Cells. Journal of Physical Chemistry C, 2015, 119, 5954-5961.	1.5	155
72	Effects of ligand exchanged CdSe quantum dot interlayer for inverted organic solar cells. Organic Electronics, 2015, 25, 44-49.	1.4	16

#	Article	IF	CITATIONS
73	Self-Organized Formation of Embossed Nanopatterns on Various Metal Substrates: Application to Flexible Solar Cells. Electrochimica Acta, 2015, 176, 636-641.	2.6	1
74	Enhanced performance of layer-evolved bulk-heterojunction solar cells with Ag nanoparticles by sequential deposition. Organic Electronics, 2015, 24, 325-329.	1.4	8
75	The effect of processing additives for charge generation, recombination, and extraction in bulk heterojunction layers of all-polymer photovoltaics. Applied Physics Letters, 2015, 107, 063302.	1.5	5
76	Structure–Property Correlation: A Comparison of Charge Carrier Kinetics and Recombination Dynamics in All-Polymer Solar Cells. Journal of Physical Chemistry C, 2015, 119, 26311-26318.	1.5	9
77	Dispersion control of Ag nanoparticles in bulk-heterojunction for efficient organic photovoltaic devices. Organic Electronics, 2015, 16, 118-125.	1.4	9
78	Enhanced Fill Factor of Tandem Organic Solar Cells Incorporating a Diketopyrrolopyrroleâ€Based Lowâ€Bandgap Polymer and Optimized Interlayer. ChemSusChem, 2015, 8, 331-336.	3.6	8
79	Tailoring Dispersion and Aggregation of Au Nanoparticles in the BHJ Layer of Polymer Solar Cells: Plasmon Effects versus Electrical Effects. ChemSusChem, 2014, 7, 3452-3458.	3.6	12
80	Efficient solution-processed small-molecule solar cells by insertion of graphene quantum dots. Nanoscale, 2014, 6, 15175-15180.	2.8	30
81	Roles of solvent additive in organic photovoltaic cells through intensity dependence of current-voltage characteristics and charge recombination. Applied Physics Letters, 2014, 105, .	1.5	7
82	Effects of Solvent Additives on Morphology, Charge Generation, Transport, and Recombination in Solutionâ€Processed Smallâ€Molecule Solar Cells. Advanced Energy Materials, 2014, 4, 1301469.	10.2	194
83	Enhanced Power Conversion Efficiency of Low Bandâ€Gap Polymer Solar Cells by Insertion of Optimized Binary Processing Additives. Advanced Energy Materials, 2014, 4, 1300835.	10.2	40
84	Effect of processing additive on morphology and charge extraction in bulk-heterojunction solar cells. Journal of Materials Chemistry A, 2014, 2, 15052-15057.	5.2	39
85	Enhanced Performance and Stability of Polymer BHJ Photovoltaic Devices from Dry Transfer of PEDOT:PSS. ChemSusChem, 2014, 7, 1957-1963.	3.6	23
86	Efficient Hole Extraction from Sb ₂ S ₃ Heterojunction Solar Cells by the Solid Transfer of Preformed PEDOT:PSS Film. Journal of Physical Chemistry C, 2014, 118, 22672-22677.	1.5	24
87	Tailoring of the plasmonic and waveguide effect in bulk-heterojunction photovoltaic devices with ordered, nanopatterned structures. Organic Electronics, 2014, 15, 3120-3126.	1.4	3
88	Sub-100nm scale polymer transfer printing process for organic photovoltaic devices. Solar Energy Materials and Solar Cells, 2013, 109, 1-7.	3.0	7
89	Balancing Light Absorptivity and Carrier Conductivity of Graphene Quantum Dots for High-Efficiency Bulk Heterojunction Solar Cells. ACS Nano, 2013, 7, 7207-7212.	7.3	171
90	Transferable Graphene Oxide by Stamping Nanotechnology: Electronâ€Transport Layer for Efficient Bulkâ€Heterojunction Solar Cells. Angewandte Chemie - International Edition, 2013, 52, 2874-2880.	7.2	112

#	Article	IF	CITATIONS
91	Layer-by-Layer All-Transfer-Based Organic Solar Cells. Langmuir, 2013, 29, 5377-5382.	1.6	22
92	Efficient Solutionâ€Processed Smallâ€Molecule Solar Cells with Inverted Structure. Advanced Materials, 2013, 25, 2397-2402.	11.1	480
93	Enhanced Efficiency Parameters of Solutionâ€Processable Smallâ€Molecule Solar Cells Depending on ITO Sheet Resistance. Advanced Energy Materials, 2013, 3, 1161-1165.	10.2	94
94	Barium: An Efficient Cathode Layer for Bulk-heterojunction Solar Cells. Scientific Reports, 2013, 3, 1965.	1.6	353
95	Polymer Bulk Heterojunction Solar Cells with PEDOT:PSS Bilayer Structure as Hole Extraction Layer. ChemSusChem, 2013, 6, 1070-1075.	3.6	26
96	Intensity Dependence of Current–Voltage Characteristics and Recombination in High-Efficiency Solution-Processed Small-Molecule Solar Cells. ACS Nano, 2013, 7, 4569-4577.	7.3	857
97	Improved Light Harvesting and Improved Efficiency by Insertion of an Optical Spacer (ZnO) in Solution-Processed Small-Molecule Solar Cells. Nano Letters, 2013, 13, 3796-3801.	4.5	554
98	Discrepancy of Optimum Ratio in Bulk Heterojunction Photovoltaic Devices: Initial Cell Efficiency vs Long-Term Stability. ACS Applied Materials & Interfaces, 2013, 5, 1612-1618.	4.0	12
99	Electron and hole mobility in solution-processed small molecule-fullerene blend: Dependence on the fullerene content. Applied Physics Letters, 2013, 102, 163308.	1.5	15
100	Additiveâ€Free Bulkâ€Heterojuction Solar Cells with Enhanced Power Conversion Efficiency, Comprising a Newly Designed Selenopheneâ€Thienopyrrolodione Copolymer. Advanced Functional Materials, 2013, 23, 1297-1304.	7.8	93
101	Polymer Solar Cells: Efficiency Increase in Flexible Bulk Heterojunction Solar Cells with a Nanoâ€Patterned Indium Zinc Oxide Anode (Adv. Energy Mater. 11/2012). Advanced Energy Materials, 2012, 2, 1282-1282.	10.2	1
102	Stamping Transfer of a Quantum Dot Interlayer for Organic Photovoltaic Cells. Langmuir, 2012, 28, 9893-9898.	1.6	24
103	Enhanced light harvesting in bulk heterojunction photovoltaic devices with shape-controlled Ag nanomaterials: Ag nanoparticles versus Ag nanoplates. RSC Advances, 2012, 2, 7268.	1.7	57
104	Efficiency Increase in Flexible Bulk Heterojunction Solar Cells with a Nanoâ€Patterned Indium Zinc Oxide Anode. Advanced Energy Materials, 2012, 2, 1319-1322.	10.2	40
105	Hematite modified tungsten trioxide nanoparticle photoanode for solar water oxidation. Journal of Power Sources, 2012, 210, 32-37.	4.0	39
106	Stability comparison: A PCDTBT/PC71BM bulk-heterojunction versus a P3HT/PC71BM bulk-heterojunction. Solar Energy Materials and Solar Cells, 2012, 101, 249-255.	3.0	49
107	The role of non-solvent swelling in bulk hetero junction solar cells. Solar Energy Materials and Solar Cells, 2012, 102, 196-200.	3.0	10
108	Efficient and low potential operative host/guest concentration graded bilayer polymer electrophosphorescence devices. Journal of Luminescence, 2012, 132, 870-874.	1.5	3

#	Article	IF	CITATIONS
109	Analysis of surface morphological changes in organic photovoltaic devices: bilayer versus bulk-heterojunction. Energy and Environmental Science, 2011, 4, 1434.	15.6	21
110	Controlled Synthesis of Vertically Aligned Hematite on Conducting Substrate for Photoelectrochemical Cells: Nanorods versus Nanotubes. ACS Applied Materials & Interfaces, 2011, 3, 1852-1858.	4.0	100
111	Sequential Processing: Control of Nanomorphology in Bulk Heterojunction Solar Cells. Nano Letters, 2011, 11, 3163-3168.	4.5	114
112	Enhanced Power Conversion Efficiency in PCDTBT/PC ₇₀ BM Bulk Heterojunction Photovoltaic Devices with Embedded Silver Nanoparticle Clusters. Advanced Energy Materials, 2011, 1, 766-770.	10.2	242
113	Rücktitelbild: Enhancement of Donor-Acceptor Polymer Bulk Heterojunction Solar Cell Power Conversion Efficiencies by Addition of Au Nanoparticles (Angew. Chem. 24/2011). Angewandte Chemie, 2011, 123, n/a-n/a.	1.6	0
114	Enhancement of Donor–Acceptor Polymer Bulk Heterojunction Solar Cell Power Conversion Efficiencies by Addition of Au Nanoparticles. Angewandte Chemie - International Edition, 2011, 50, 5519-5523.	7.2	334
115	Back Cover: Enhancement of Donor-Acceptor Polymer Bulk Heterojunction Solar Cell Power Conversion Efficiencies by Addition of Au Nanoparticles (Angew. Chem. Int. Ed. 24/2011). Angewandte Chemie - International Edition, 2011, 50, 5404-5404.	7.2	2
116	The effect of a concentration graded cathode for organic solar cells. Solar Energy Materials and Solar Cells, 2011, 95, 2443-2447.	3.0	8
117	Roles of Interlayers in Efficient Organic Photovoltaic Devices. Macromolecular Rapid Communications, 2010, 31, 2095-2108.	2.0	92
118	Effect of the ordered 2D-dot nano-patterned anode for polymer solar cells. Organic Electronics, 2010, 11, 285-290.	1.4	30
119	Active layer transfer by stamping technique for polymer solar cells: Synergistic effect of TiOx interlayer. Organic Electronics, 2010, 11, 599-603.	1.4	22
120	Unexpected solid–solid intermixing in a bilayer of poly(3-hexylthiophene) and [6,6]-phenyl C61-butyric acidmethyl ester via stamping transfer. Organic Electronics, 2010, 11, 1376-1380.	1.4	37
121	Enhanced charge collection via nanoporous morphology in polymer solar cells. Applied Physics Letters, 2010, 96, 103304.	1.5	12
122	Photovoltaic Devices with an Active Layer from a Stamping Transfer Technique: Single Layer Versus Double Layer. Langmuir, 2010, 26, 9584-9588.	1.6	38
123	Dye-sensitized solar cells with Pt- and TCO-free counter electrodes. Chemical Communications, 2010, 46, 4505.	2.2	172
124	Solution-processable polymer based photovoltaic devices with concentration graded bilayers made via composition control of a poly(3-hexylthiophene)/[6,6]-phenyl C61-butyric acidmethyl ester. Journal of Materials Chemistry, 2010, 20, 4910.	6.7	25
125	Enhanced High-Temperature Long-Term Stability of Polymer Solar Cells with a Thermally Stable TiOx Interlayer. Journal of Physical Chemistry C, 2009, 113, 17268-17273.	1.5	60
126	Solution-processable polymer solar cells from a poly(3-hexylthiophene)/[6,6]-phenyl C61-butyric acidmethyl ester concentration graded bilayers. Applied Physics Letters, 2009, 95, 043505.	1.5	62